



# Co(II)<sub>4</sub>Gd(III)<sub>6</sub> phosphonate grid and cage as molecular refrigerants



Xiaoyan Tang, Qixuan Zhong, Ji Xu, Haiqing Li, Sinong Xu, Xueyuan Cui, Bo Wei\*, Yunsheng Ma\*, Rongxin Yuan\*

Key Laboratory of Advanced Functional Materials, School of Chemistry & Materials Engineering, Changshu Institute of Technology, Changshu 215500, PR China

## ARTICLE INFO

### Article history:

Received 4 October 2015  
Received in revised form 29 November 2015  
Accepted 1 December 2015  
Available online 23 December 2015

### Keywords:

Co–Gd  
Cage  
Phosphonate  
Molecular refrigerant

## ABSTRACT

The study on structure–property relationships of polynuclear 3d–Gd clusters are very essential in the fields of magnetic refrigerants. We designed two new bulky phosphonic acids: (3-(9H-carbazol-9-yl)propyl)phosphonic acid (CarbpPO<sub>3</sub>H<sub>2</sub>) and (2-(9-methyl-9H-fluoren-9-yl)ethyl)phosphonic acid (FlumePO<sub>3</sub>H<sub>2</sub>). Based on these ligands, two clusters [Co(II)<sub>4</sub>Gd(III)<sub>6</sub>(CarbpPO<sub>3</sub>)<sub>6</sub>(<sup>t</sup>BuCO<sub>2</sub>)<sub>14</sub>(<sup>t</sup>BuCO<sub>2</sub>H)(H<sub>2</sub>O)<sub>3</sub>]·9CH<sub>3</sub>CN·CH<sub>2</sub>Cl<sub>2</sub> (**1**) and [Co(II)<sub>4</sub>Gd(III)<sub>6</sub>(FlumePO<sub>3</sub>)<sub>3</sub>(<sup>t</sup>BuCO<sub>2</sub>)<sub>14</sub>(μ<sub>3</sub>-OH)<sub>6</sub>(H<sub>2</sub>O)<sub>2</sub>(CH<sub>3</sub>CN)]·6CH<sub>3</sub>CN (**2**) were synthesized under ambient condition. Compound **1** has a [3 × 3] grid-like structure, while compound **2** has a rare helmet-like cage structure. The magnetocaloric effect (MCE) have been tuned from 22.83 to 29.06 J kg<sup>-1</sup> K<sup>-1</sup> as the molecular structure changes from grid to cage.

© 2015 Elsevier B.V. All rights reserved.

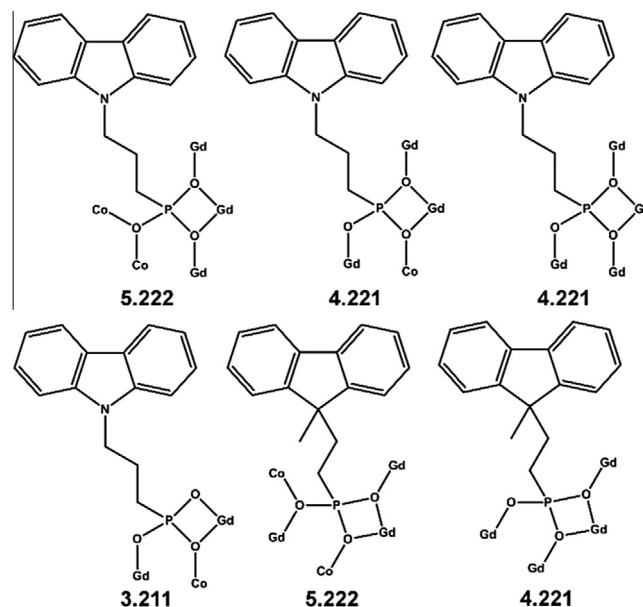
## 1. Introduction

Molecular clusters have received a great deal attention due to their potential applications in magnetic science such as single-molecule magnets (SMMs) and magnetic refrigerants [1,2]. The latter are based on the magnetocaloric effect (MCE), where an adiabatic demagnetization process leads to cooling [3]. Since the observation of MCE in Mn<sub>12</sub> and Fe<sub>8</sub> clusters, molecule-based magnetic refrigerants have been a hot research topic and rapidly developing for their synthetic and functional tunability [4]. However, to increase the MCE of clusters is still a great challenge.

Phosphonic acid of the general formula RPO<sub>3</sub>H<sub>2</sub> (R = alkyl or aryl) have been proved to be ideal for the construction of molecular clusters [5]. Interestingly, the 3d–4f phosphonate clusters could function as magnetic refrigerants [6]. To date, the strategy focusing on metal ions has been reported to increase the MCE of the clusters. Such as, utilizing ferromagnetic interactions between metal ions and incorporation of the negligible magnetic anisotropy of Gd(III) ion to build Ni–Gd clusters [7]. Employing both isotropic and higher spins of Mn(II) and Gd(III) ions to build Mn–Gd clusters [8]. Increasing the percentage of the Gd(III) ions in the Co–Gd clusters to increase the MCE of the clusters [9].

We deem that reducing the ratio of organic ligands in a cluster with different inorganic components would be feasible to increase the MCE [10]. As for we have found the R groups in RPO<sub>3</sub>H<sub>2</sub> play a key role for the formation of the phosphonate clusters [11], then

we designed the carbazolyl and fluorenyl phosphonate ligands to construct Co–Gd clusters to tune MCE. Fortunately, we obtained two Co<sub>4</sub>Gd<sub>6</sub> clusters with distinct structures and molecular weight, thus we think this could provide us a platform to study the light molecular weight on the tuning of MCE.



**Scheme 1.** Coordination modes of the phosphonates. Labeled with Harris Notation [12].

\* Corresponding authors.

E-mail addresses: myschem@hotmail.com (Y. Ma), yuanrx@csg.edu.cn (R. Yuan).

## 2. Experimental section

### 2.1. Materials and methods

[Co<sub>2</sub>(μ-OH)<sub>2</sub>(<sup>t</sup>BuCO<sub>2</sub>)<sub>2</sub>(<sup>t</sup>BuCO<sub>2</sub>H)<sub>4</sub>] **Co**<sub>2</sub> [13], [Co<sub>9</sub>(<sup>t</sup>BuCO<sub>2</sub>H)<sub>4</sub>(O)<sub>3</sub>(OH)<sub>3</sub>(<sup>t</sup>BuCO<sub>2</sub>)<sub>12</sub>] **Co**<sub>9</sub> [14], and [Gd<sub>2</sub>(<sup>t</sup>BuCO<sub>2</sub>)<sub>6</sub>(<sup>t</sup>BuCO<sub>2</sub>H)<sub>6</sub>] **Gd**<sub>2</sub> [9] were prepared according to the literature methods. (3-(9H-carbazol-9-yl)propyl)phosphonic acid (CarbpPO<sub>3</sub>H<sub>2</sub>) and (2-(9-methyl-9H-fluoren-9-yl)ethyl)phosphonic acid (FlumePO<sub>3</sub>H<sub>2</sub>) were prepared as described in ESI. All other chemicals and solvents were commercially purchased and used as received. Elemental analyses (EA) were performed on a PE 240C elemental analyzer. The IR spectra were recorded on a NICOLET 380 spectrometer with pressed KBr pellets. All the magnetic studies were performed on microcrystalline state. The magnetic susceptibilities were measured on a Quantum Design MPMS SQUID-XL7 magnetometer. Diamagnetic corrections were made for both the sample holder and the compounds estimated from Pascal's constants [15].

#### 2.1.1. Synthesis of [Co(II)<sub>4</sub>Gd(III)<sub>6</sub>(CarbpPO<sub>3</sub>)<sub>6</sub>(<sup>t</sup>BuCO<sub>2</sub>)<sub>14</sub>(<sup>t</sup>BuCO<sub>2</sub>H)(H<sub>2</sub>O)<sub>3</sub>]·9CH<sub>3</sub>CN·CH<sub>2</sub>Cl<sub>2</sub> (**1**)

Compound **1** was obtained by mixing **Co**<sub>2</sub> (0.0949 g, 0.1 mmol), **Gd**<sub>2</sub> (0.1149 g, 0.075 mmol) and CarbpPO<sub>3</sub>H<sub>2</sub> (0.0289 g, 0.1 mmol) in CH<sub>3</sub>CN/CH<sub>2</sub>Cl<sub>2</sub> (1:1) (16 mL) and stirred at room temperature for 12 h. The resulting solid was filtered and the purple solution were kept in a vial for ca. two weeks. Purple crystals were collected by filtration, yield: 0.044 g, 36% (based on **Gd**<sub>2</sub>). EA for **1**, C<sub>184</sub>H<sub>254</sub>Cl<sub>2</sub>Co<sub>4</sub>Gd<sub>6</sub>N<sub>15</sub>O<sub>51</sub>P<sub>6</sub>: C, 44.84; H, 5.20; N, 4.26. Found: C, 44.69; H, 5.01; N, 4.17%. IR (cm<sup>-1</sup>, KBr): 2962.2(m), 1540.5(vs), 1485.5(vs), 1426.3(vs), 1231.1(s), 1181.4(s), 1005.7(s), 748.6(m), 722.4(m), 612.6(m).

#### 2.1.2. Synthesis of [Co(II)<sub>4</sub>Gd(III)<sub>6</sub>(FlumePO<sub>3</sub>)<sub>3</sub>(<sup>t</sup>BuCO<sub>2</sub>)<sub>14</sub>(μ<sub>3</sub>-OH)<sub>6</sub>(H<sub>2</sub>O)<sub>2</sub>(CH<sub>3</sub>CN)]·6CH<sub>3</sub>CN (**2**)

Compound **2** was obtained by mixing **Co**<sub>9</sub> (0.1125 g, 0.05 mmol), **Gd**<sub>2</sub> (0.1149 g, 0.075 mmol) and FlumePO<sub>3</sub>H<sub>2</sub> (0.0288 g, 0.1 mmol) in CH<sub>3</sub>CN/CH<sub>2</sub>Cl<sub>2</sub> (1:1) (16 mL) and stirred at room temperature for 24 h. The resulting solid was filtered and the purple solution were kept in a vial for ca. one week. Purple crystals were collected by filtration, yield: 0.048 g, 49% (based on **Gd**<sub>2</sub>). EA for **2**, C<sub>132</sub>H<sub>202</sub>Co<sub>4</sub>Gd<sub>6</sub>N<sub>7</sub>O<sub>45</sub>P<sub>3</sub>: C, 40.87; H, 5.25; N, 2.53. Found: C, 40.65; H, 5.06; N, 2.38%. IR (cm<sup>-1</sup>, KBr): 2966.9(m), 1628.1(m), 1545.7(s), 1483.4(m), 1420.9(s), 1225.8(m), 1173.7(m), 1013.5(m), 732.8(m), 616.4(m).

### 2.2. X-ray Crystallography

Single crystals of dimensions 0.35 × 0.34 × 0.32 mm<sup>3</sup> for **1**, 0.34 × 0.33 × 0.31 mm<sup>3</sup> for **2** were used for structural determinations on a Bruker APEX-II diffractometer using graphite monochromatized Mo Kα radiation (λ = 0.71073 Å) at room temperature. Cell parameters were refined by using the program Bruker SAINT on all observed reflections. The collected data were reduced by using the program Bruker SAINT, and an absorption correction (multi-scan) was applied. The reflection data were also corrected for Lorentz and polarization effects. The structures were solved by direct methods and refined on F<sup>2</sup> by full matrix least squares using SHELXTL [16]. All of the non-hydrogen atoms were located from the Fourier maps, and were refined anisotropically. All H atoms were refined isotropically, with the isotropic vibration parameters related to the non-H atom to which they are bonded. The crystallographic and refinement details are listed in Table 1.

**Table 1**

Crystallographic data for compounds **1** and **2**.

	<b>1</b>	<b>2</b>
Formula	C <sub>184</sub> H <sub>254</sub> Cl <sub>2</sub> Co <sub>4</sub> Gd <sub>6</sub> N <sub>15</sub> O <sub>51</sub> P <sub>6</sub>	C <sub>132</sub> H <sub>202</sub> Co <sub>4</sub> Gd <sub>6</sub> N <sub>7</sub> O <sub>45</sub> P <sub>3</sub>
M	4927.96	3879.14
Crystal system	triclinic	triclinic
Space group	P $\bar{1}$	P $\bar{1}$
a (Å)	19.539(4)	17.5286(19)
b (Å)	19.715(4)	17.7822(18)
c (Å)	31.817(6)	29.359(3) Å
α (°)	84.43(3)	88.414(2)
β (°)	87.87(3)	87.751(2)
γ (°)	61.18(3)	69.2580(10)
V (Å <sup>3</sup> )	10687(4)	8550.5(15)
Z	2	2
D <sub>calc</sub> (M g m <sup>-3</sup> )	1.531	1.507
μ (mm <sup>-1</sup> )	2.281	2.767
F(000)	4974	3880
Total/unique reflections	148937/37411	116983/29837
R <sub>int</sub>	0.0789	0.0382
Goodness-of-fit (GOF) on F <sup>2</sup>	1.060	0.980
R <sub>1</sub> , wR <sub>2</sub> <sup>a</sup> [I > 2σ(I)]	0.0609, 0.1813	0.0685, 0.1896
R <sub>1</sub> , wR <sub>2</sub> (all data)	0.0937, 0.2302	0.0880, 0.2199
(Δρ) <sub>max</sub> , (Δρ) <sub>min</sub> (e Å <sup>-3</sup> )	3.345, -2.270	2.798, -1.608

$$^a R_1 = \sum ||F_o| - |F_c|| / \sum |F_o|; wR_2 = \{\sum w(F_o^2 - F_c^2)^2 / \sum w(F_o^2)\}^{1/2}.$$

## 3. Results and discussion

### 3.1. Synthesis

We have used [Gd<sub>2</sub>(<sup>t</sup>BuCO<sub>2</sub>)<sub>6</sub>(<sup>t</sup>BuCO<sub>2</sub>H)<sub>6</sub>] **Gd**<sub>2</sub> and two kinds of cobalt starting materials, the dimetallic [Co<sub>2</sub>(μ-OH)<sub>2</sub>(<sup>t</sup>BuCO<sub>2</sub>)<sub>4</sub>(<sup>t</sup>BuCO<sub>2</sub>H)<sub>4</sub>] **Co**<sub>2</sub> and nonametallc cobalt(II) [Co<sub>9</sub>(<sup>t</sup>BuCO<sub>2</sub>H)<sub>4</sub>(O)<sub>3</sub>(OH)<sub>3</sub>(<sup>t</sup>BuCO<sub>2</sub>)<sub>12</sub>] **Co**<sub>9</sub>, to react with carbazoyl and fluorenyl phosphonate ligands to produce two kinds of cluster under ambient conditions. Solvothermal conditions have been tried, however, gave dark-pink solution with some flocculation. If Gd(NO<sub>3</sub>)<sub>3</sub>·6H<sub>2</sub>O and **Co**<sub>9</sub> were used in place of **Gd**<sub>2</sub> and **Co**<sub>2</sub> in the same reaction that gives compound **1**, pale-pink block crystals can be obtained. We have measured this crystal data for many times, however, the structure cannot be fully solved due to the highly disordered organic groups. Compound **2** can also be obtained if **Co**<sub>2</sub> was used as the starting material in place of **Co**<sub>9</sub>, however, the yield is low and the crystals were very fine. The formation of different types of clusters for **1** and **2** may due to the steric hindrance of the bulky organic groups. To our knowledge, clusters **1** and **2** are rare examples of metal phosphonate clusters bearing bulky organic R groups [17].

### 3.2. Structural description

X-ray single crystal diffraction reveals that compound **1** features a grid-like structure with one Gd(III) ion surrounded by other metal centers due to the bridging phosphonates (Fig. 1). All the cobalt centers are divalent, which have been verified by the Bond Valence Sum (BVS) calculation (Table S1). Take the edge Co(II) dimer as a single node, the resulting topology is a [3 × 3] grid. In the heterometallic core, two isolated corner cobalt ions are four-coordinated with tetrahedron geometry, while cobalt sites in the Co(II) dimer are five-coordinated with a square-pyramidal geometry (τ range from 0.14 to 0.37) [18]. The Co–O and Gd–O bond lengths range from 1.914 to 2.219 Å and 2.207 to 2.752 Å, respectively, which are consistent with that observed in the Co–Gd clusters [19]. The nearest metal–metal contacts of Gd···Gd, Co···Gd

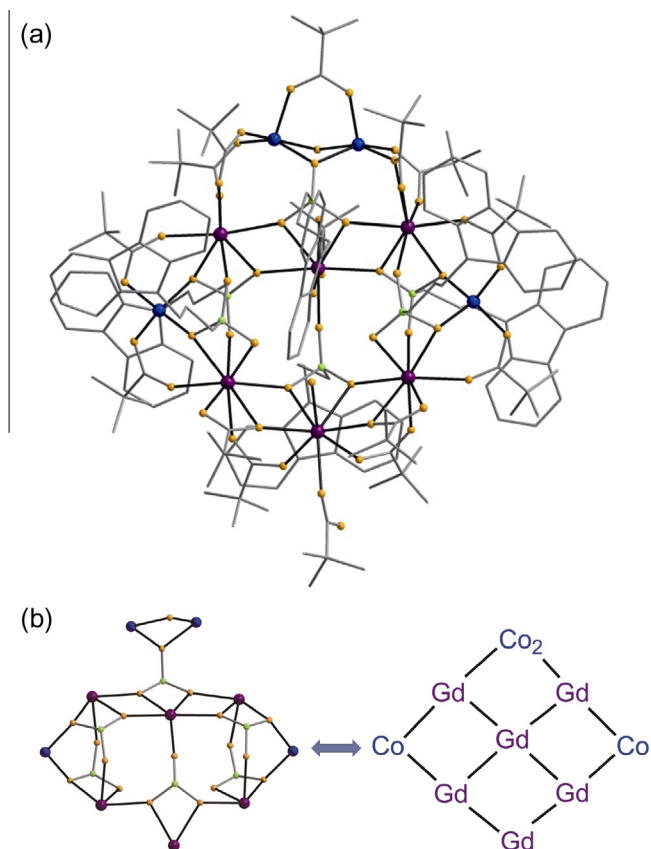


**Fig. 1.** (a) The structure of **1** in the crystal. Color codes: blue, cobalt; purple, lanthanide; green, phosphorous; yellow, oxygen; gray, carbon; hydrogen atoms and lattice solvent molecules are omitted for clarity. (b) The comparison of the core of **1** (left) and the [3 × 3] {Co<sub>4</sub>Gd<sub>6</sub>} grid (right) by taking the cobalt dimer as a node. (For interpretation of the references to colour in this figure legend, the reader is referred to the web version of this article.)

and Co···Co contacts are 3.92, 3.76 and 3.10 Å, respectively. The phosphonates show 5.222, 4.221 and 3.211 coordination modes in **1**. Fourteen deprotonated pivalates are surrounded in 2.11 mode in the periphery (see Scheme 1). There exists a protonated pivalic acid coordinating with Gd atom in 1.10 mode. The inorganic core was surrounded by the strongly hydrophilic carbazolyl and tert-butyl groups from phosphonates and pivalates. It should be noted that this grid-like core structure is similar to that in [Mn<sub>4</sub>Gd<sub>6</sub>(O<sub>3</sub>PCH<sub>2</sub>Ph)<sub>6</sub>(HO<sub>2</sub>CtBu)<sub>3</sub>(O<sub>2</sub>CMe)(HO<sub>2</sub>C<sup>t</sup>Bu)(OH)<sub>2</sub>(MeCN)<sub>2</sub>] and [Co<sub>4</sub>Dy<sub>6</sub>(O<sub>3</sub>PCH<sub>2</sub>Ph)<sub>6</sub>(O<sub>2</sub>C<sup>t</sup>Bu)<sub>14</sub>(HO<sub>2</sub>C<sup>t</sup>Bu)(MeCN)(H<sub>2</sub>O)<sub>2</sub>] with PhCH<sub>2</sub>PO<sub>3</sub>H<sub>2</sub> and HO<sub>2</sub>C<sup>t</sup>Bu ligands [8,9]. Fig. S1 shows the packing diagram of compound **1** along the *a*-axis. Clearly, the decanuclear molecules are stacked in the lattice, forming vacancies where the lattice molecules reside. The  $\pi$ - $\pi$  stacking interaction is found between the molecules with centroid-centroid distance between the carbazolyl groups of 4.46 Å [20].

Compound **2** has a helmet-like cage structure due to the bridging phosphonates, pivalates and  $\mu_3$ -OH groups (Fig. 2). The helmet can be described as one cobalt atom locates on the top position, two Gd<sub>2</sub>O<sub>2</sub> rhombuses sit on the earmuff sites with each connected with another cobalt atom, one CoGdO<sub>2</sub> rhombus lies on the visor site, and one Gd atom locates on the back of the head. Earmuffs and visor are joined together by three phosphonate groups, while the top, earmuffs and visor are connected by  $\mu_3$ -OH groups. The cage contains two four-coordinate cobalt ions with tetrahedral coordination geometries. While, the last two cobalt sites are six and five-coordinate with octahedral and square-pyramidal geometries. All the cobalt centers are divalent according to the Bond

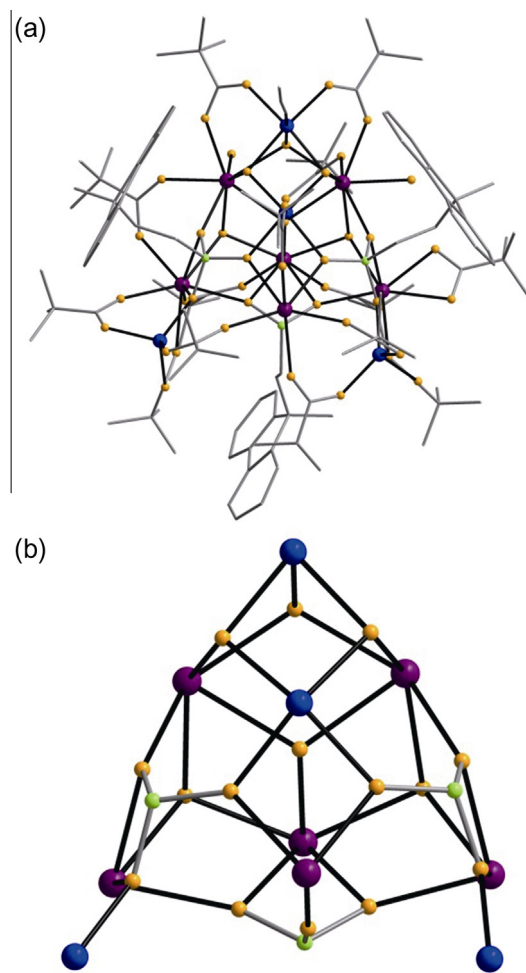


**Fig. 2.** (a) The structure of **2** in the crystal. Color codes are the same to compound **1**. Lattice solvent molecules are omitted for clarity. (b) Helmet-like core of **2**. (For interpretation of the references to colour in this figure legend, the reader is referred to the web version of this article.)

Valence Sum (BVS) calculation (Table S2). Two phosphonates in the cage show 5.222 mode to coordinate with Co and Gd atoms, while the third one shows 4.221 mode to coordinate with four Gd atoms. Fourteen deprotonated pivalates are surrounded in the periphery in 2.11 or 1.11 modes. The Co–O and Gd–O bond lengths lie in the ranges of 1.934–2.156 Å and 2.207–2.752 Å, respectively. The nearest Gd···Gd, Co···Gd and Co···Co separations are 3.95, 3.70 and 3.12 Å, respectively, which are similar to that in compound **1**. The exterior of the cage consists of fluorenyl and tert-butyl groups from the ligands, leading to a hydrophobic exterior. The molecules are stacked in the lattice, forming vacancies to fill the guest molecules (Fig. S2).

### 3.3. Magnetic properties

The magnetic behavior of **1** and **2** were studied on polycrystalline samples using a SQUID magnetometer (Fig. 3). At room temperature the  $\chi T$  values (64.5 cm<sup>3</sup> K mol<sup>-1</sup> for **1**, 62.7 cm<sup>3</sup> K mol<sup>-1</sup> for **2**) are larger than the calculated spin-only value (54.75 cm<sup>3</sup> K mol<sup>-1</sup> for four *S* = 3/2 and six *S* = 7/2 centers, *g* = 2). The differences are due to orbital contributions from Co(II) ions [15]. Upon cooling, for **1**, the  $\chi T$  decreases slowly with decreasing temperature down to about 50 K, before decreasing more rapidly. At 1.8 K the  $\chi T$  is 43.0 cm<sup>3</sup> K mol<sup>-1</sup>, indicating paramagnetic states are still populated due to the very weak exchange involving

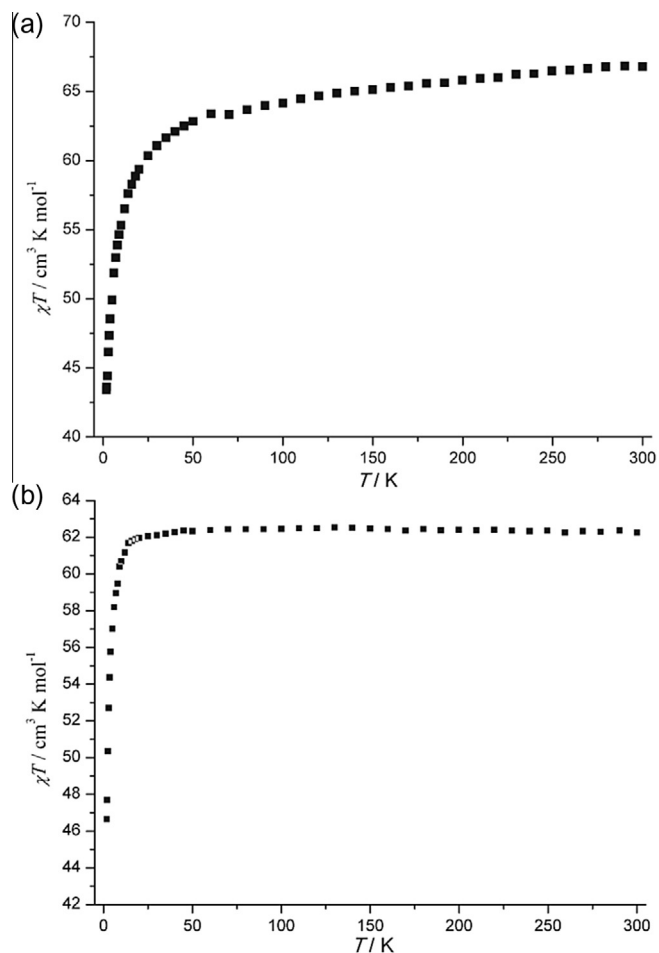


Fig. 3. The  $\chi T$  versus  $T$  plot of **1** (a) and **2** (b) under 0.1 T dc field.

4f-ions. The quench of the orbital-contribution also contributes to the decrease of  $\chi T$  with lowering the temperature because of the tetra- and pentacoordinated Co(II). For **2**,  $\chi T$  remains nearly unchanged down to 16 K, this reflects a very weak magnetic interaction between the metal centers. Upon cooling,  $\chi T$  decreases sharply to  $46.6 \text{ cm}^3 \text{ K mol}^{-1}$  at 1.8 K, indicating a paramagnetic state still present. Magnetization measurements were performed in the range of 0–7 T at 2 K (Figs. S3 and S4). The  $M$  values show a steady increase with increasing field to 55.4 and  $55.3 \text{ N}\beta$  at 7 T without achieving saturation. The quantitative analysis was not performed given the complexity of the structures and the orbital degenerate nature of the cobalt ions.

The magnetocaloric properties were investigated. The magnetic entropy changes for changing applied field were calculated indirectly from the magnetization behavior as a function of applied field and temperature (Fig. 4) using the standard relationship  $\Delta S = \int [\partial M(T, H) / \partial T]_H dH$  [21]. For **1**, the  $-\Delta S$  versus  $T$  plots increase gradually from 10 to 2 K, reaching a maximum of  $22.83 \text{ J kg}^{-1} \text{ K}^{-1}$  at 7 T. The observed value is close to that reported for  $\{\text{Co}_4\text{Gd}_6\}$  [9]. There is no sign of a downturn, which means the maximum should come at a lower temperature for the investigated applied field changes. For **2**, the  $-\Delta S$  versus  $T$  plots reach a maximum of  $29.06 \text{ J kg}^{-1} \text{ K}^{-1}$  at 2 K. This entropy change is slightly higher than the reported ( $28.6 \text{ J kg}^{-1} \text{ K}^{-1}$ ) of the  $\{\text{Co}_6\text{Gd}_8\}$  cage [9]. Take a comparison of entropy exchanges of **1**, **2** and the reported  $\{\text{Co(II)}_4\text{Gd(III)}_6\}$  cluster, we can draw a conclusion that the larger MCE exhibited by compound **2** is own to its light molecular weight.

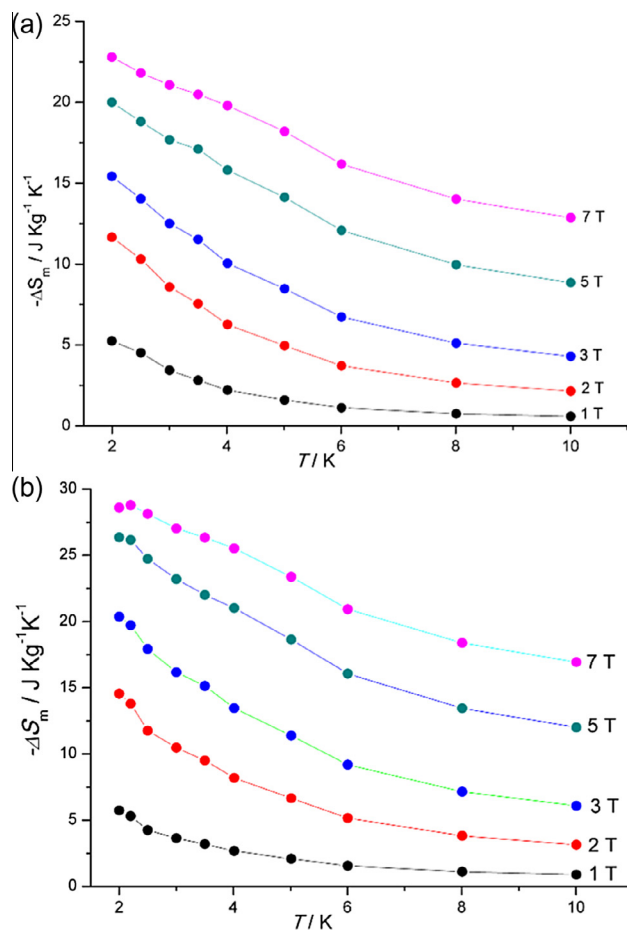


Fig. 4. Experimental  $\Delta S_m$  for **1** (a) and **2** (b) at various fields and temperatures. Lines are guides to the eye.

#### 4. Conclusions

The preparation of grid and helmet-like  $\{\text{Co(II)}_4\text{Gd(III)}_6\}$  clusters by employing bulky phosphonate ligands was performed. The results show that both starting metal sources and bulky carbazoly/fluorenyl ligands are responsible for the isolation of these clusters. The helmet-like  $\{\text{Co(II)}_4\text{Gd(III)}_6\}$  shows light molecular weight compared with the grid-like one, which is advantageous to magnetic refrigerants. The observation of a larger MCE in **2** means our strategy of tuning MCE by designing the cluster with light molecular weight is practicable. In addition, our studies on Co–Gd clusters bearing carbazoly/fluorenyl phosphonate ligands should be advantageous since 3d ions and a wide variety of ligands are available. Further studies on Mn–Gd clusters for magnetic refrigeration are underway based on the carbazoly/fluorenyl phosphonate ligands.

#### Acknowledgements

This work is supported by NSFC (Nos. 20101018, 21201025) and NSF of Jiangsu Province (Nos. BK2012643, BK2012210, 12KJA150001, 14KJA150001).

#### Appendix A. Supplementary material

CCDC 1417642 and 1417643 contain the supplementary crystallographic data for compounds **1** and **2**. These data can be obtained free of charge from The Cambridge Crystallographic Data

Centre via [www.ccdc.cam.ac.uk/data\\_request/cif](http://www.ccdc.cam.ac.uk/data_request/cif). Supplementary data associated with this article can be found, in the online version, at <http://dx.doi.org/10.1016/j.ica.2015.12.013>.

## References

- [1] (a) L. Ungur, S.-Y. Lin, J. Tang, L. Chibotaru, *Chem. Soc. Rev.* 43 (2014) 6894; (b) D.N. Woodruff, R.E.P. Winpenny, R.A. Layfield, *Chem. Rev.* 113 (2013) 5110.
- [2] (a) Y.-Z. Zheng, G.-J. Zhou, Z. Zheng, R.E.P. Winpenny, *Chem. Soc. Rev.* 43 (2014) 1462; (b) G. Karotsis, M. Evangelisti, S.J. Dalgarno, E.K. Brechin, *Angew. Chem., Int. Ed.* 48 (2009) 9928.
- [3] Y.I. Spichkin, A.K. Zvezdin, S.P. Gubin, A.S. Mischenko, A.M. Tishin, *J. Phys. D Appl. Phys.* 34 (2001) 1162.
- [4] (a) F. Torres, J.M. Hernández, X. Bohigas, J. Tejada, *Appl. Phys. Lett.* 77 (2000) 3248; (b) X.X. Zhang, H.L. Wei, Z.Q. Zhang, L. Zhang, *Phys. Rev. Lett.* 87 (2001) 157203; (c) J.-L. Liu, Y.-C. Chen, F.-S. Guo, M.-L. Tong, *Coord. Chem. Rev.* 281 (2014) 26.
- [5] J. Goura, V. Chandrasekhar, *Chem. Rev.* 115 (2015) 6854.
- [6] V. Baskar, K. Gopal, M. Helliwell, F. Tuna, W. Wernsdorfer, R.E.P. Winpenny, *Dalton Trans.* 39 (2010) 4747.
- [7] (a) Y.Z. Zheng, M. Evangelisti, R.E.P. Winpenny, *Angew. Chem., Int. Ed.* 50 (2011) 3692; (b) E.M. Pineda, F. Tuna, Y.-Z. Zheng, R.E.P. Winpenny, E.J.L. McInnes, *Inorg. Chem.* 52 (2013) 13702.
- [8] Y.Z. Zheng, E.M. Pineda, M. Helliwell, R.E.P. Winpenny, *Chem. Eur. J.* 18 (2012) 4146.
- [9] (a) Y.Z. Zheng, M. Evangelisti, R.E.P. Winpenny, *Chem. Sci.* 2 (2011) 99; (b) Y.Z. Zheng, M. Evangelisti, F. Tuna, R.E.P. Winpenny, *J. Am. Chem. Soc.* 134 (2012) 1057.
- [10] Y.C. Chen, F.S. Guo, Y.Z. Zheng, J.L. Liu, J.D. Leng, R. Tarasenko, M. Orendáč, J. Prokleška, V. Sechovský, M.L. Tong, *Chem. Eur. J.* 19 (2013) 13504.
- [11] (a) Y.S. Ma, Y. Song, Y.Z. Li, L.M. Zheng, *Inorg. Chem.* 46 (2007) 5459; (b) Y.S. Ma, Y.Z. Li, Y. Song, L.M. Zheng, *Inorg. Chem.* 47 (2008) 4536; (c) Y.S. Ma, Y. Song, X.Y. Tang, R.X. Yuan, *Dalton Trans.* 39 (2010) 6262; (d) H.C. Yao, Y.Z. Li, Y. Song, Y.S. Ma, L.M. Zheng, X.Q. Xin, *Inorg. Chem.* 45 (2006) 59; (e) Y.S. Ma, H.C. Yao, W.J. Hua, S.H. Li, Y.Z. Li, L.M. Zheng, *Inorg. Chim. Acta* 360 (2007) 1645–1650.
- [12] Harris notation describes the binding mode as, *J. Chem. Soc., Dalton Trans.* (2000) 2349.
- [13] G. Chaboussant, R. Basler, H.-U. Gudel, S.T. Oxsenbein, A. Parkin, S. Parsons, G. Rajaraman, A. Sieber, A.A. Smith, G.A. Timco, R.E.P. Winpenny, *Dalton Trans.* (2004) 2758.
- [14] D.A. Brown, W.K. Glass, N.J. Fitzpatrick, T.J. Kemp, W. Errington, G.J. Clarkson, W. Hasse, F. Karsten, A.H. Mahdy, *Inorg. Chim. Acta* 357 (2004) 1411.
- [15] O. Kahn, *Molecular Magnetism*, VCH Publishers Inc., New York, 1993.
- [16] G.M. Sheldrick, *Acta Crystallogr. Sect. A Found. Crystallogr.* 64 (2008) 112.
- [17] (a) V. Baskar, M. Shanmugam, E.C. Sanudo, M. Shanmugam, D. Collison, E.J.L. McInnes, Q. Wei, R.E.P. Winpenny, *Chem. Commun.* (2007) 37; (b) Y.S. Ma, W.S. Cai, B. Chen, J.Y. Chang, X.Y. Tang, R.X. Yuan, *CrystEngComm* 15 (2013) 7615.
- [18] A.W. Addison, T.N. Rao, J. Reedijk, J. van Rijn, G.C. Verschoor, *J. Chem. Soc., Dalton Trans.* (1984) 1349.
- [19] E.M. Pineda, F. Tuna, R.G. Pritchard, A.C. Regan, R.E.P. Winpenny, E.J.L. McInnes, *Chem. Commun.* 49 (2013) 3522.
- [20] C. Janiak, *J. Chem. Soc., Dalton Trans.* (2000) 3885.
- [21] V.K. Pecharsky, K.A. Gschneidner Jr., *J. Magn. Magn. Mater.* 200 (1999) 44.